0.1 Beam-beam effects, parameter choices, and luminosity

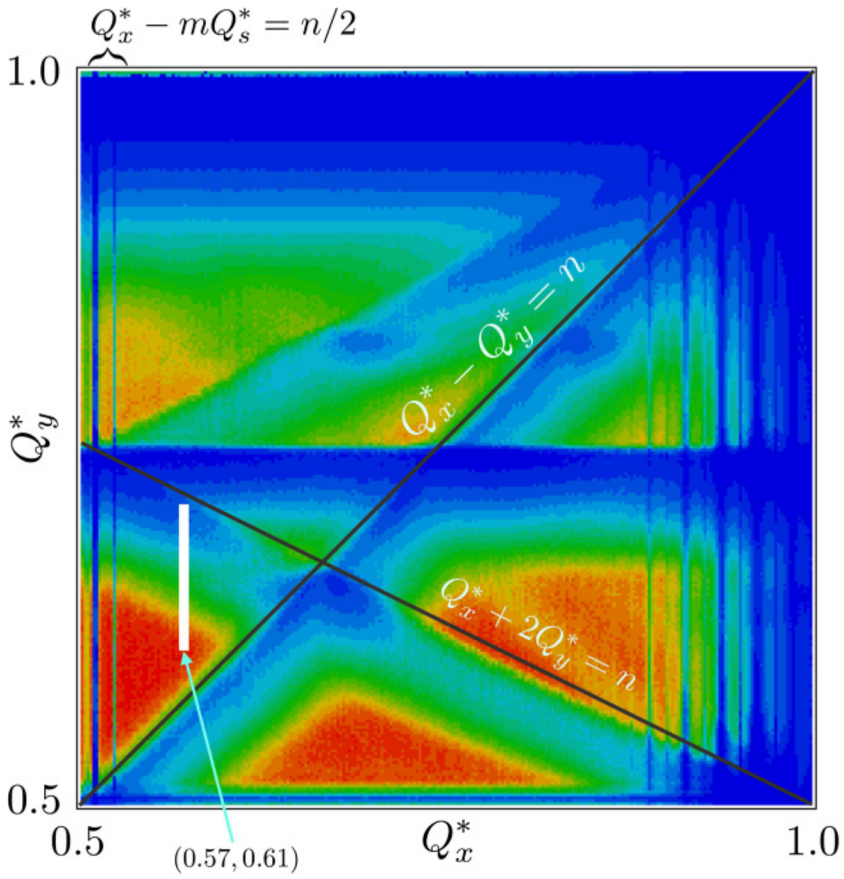

Fig. 1: Luminosity at Z as a function of betatron tunes for the CDR configuration [**?**]. The colour scale from zero (blue) to $2.3 \cdot 10^{36}$ cm^{2}s^1 (red). The white narrow rectangle above (0.57, 0.61) shows the footprint due to the beam-beam interaction.

Following encouraging experience at DAΦNE and SuperKEKB, the FCC-ee is based on the so-called crab waist scheme. It features very flat beams ($\sigma_x^* \gg \sigma_y^*$), a large crossing angle between the beams and crab sextupoles at each side of the IPs allowing to maintain a good stability of the particles trajectories even when the beam-beam interaction is strong, thus allowing for a high luminosity. In this regime, the luminosity may be expressed as follows:

$$\mathcal{L} = \frac{\gamma}{2er_e}\frac{I_{tot}\xi_y}{\beta_y^*}R_{HG} \tag{1}$$

with the relativistic factor γ, the elementary charge e, the classical electron radius r_e, the total beam current I_{tot}, the vertical beam-beam parameter ξ_y, the vertical optical β function at the IP β_y^* and the hourglass reduction factor R_{HG}. The total current is constrained by the design choice of limiting the emitted synchrotron radiation power to 50 MW per beam. The highest vertical beam-beam parameter is therefore desired. In order to maintain the tune footprint away from low order resonance all configurations feature $\xi_y \approx 0.1$ (Fig. 1). The smallest β_y^* is also desired, yet it is limited by the reduction of the luminosity by the hourglass effect, leading to the condition $\beta_y^* \approx L_i$, the interaction length defined as:

$$L_i = \frac{\sigma_z}{\sqrt{1+\phi^2}},\ \phi = \frac{\sigma_z}{\sigma_x}\tan\left(\frac{\theta}{2}\right) \tag{2}$$

with the horizontal and longitudinal beam sizes $\sigma_{x,z}$, the so-called Piwinski angle ϕ related to the full crossing angle between the beams at the IP θ. Considering the small angle approximation ($\theta \ll 1$)

and the large Piwniski angle case ($\phi \gg 1$), then the interaction length reduces to $2\sigma_x/\theta$. The crossing angle θ is imposed by the choice of layout, in particular due to the short common chamber around the IP specifically designed to avoid parasitic beam-beam encounters. In order to maximise the luminosity it is therefore favourable to minimise the horizontal beam size in order to allow for a reduction of β_y^*, yet it is important to keep in mind that the β_y^* is eventually limited due to the impact of the corresponding chromatic correction on dynamic aperture. At this point $\beta^*_{y,min} = 0.7$ mm is considered acceptable for Z and slightly higher for higher energies (Chap. **??**), thus constraining the horizontal beam size at the IP $\sigma_x \gtrapprox \beta^*_{y,min}\theta/2$.
The beam-beam tune shifts are given by

$$\xi_x = \frac{N_b r_e}{2\pi\gamma}\frac{\beta_x^*}{\sigma_x^2(1+\phi^2)},\ \xi_y = \frac{N_b r_e}{2\pi\gamma}\frac{\beta_y^*}{\sigma_x\sigma_y(1+\phi^2)} \tag{3}$$

with N_b the number of electron or positron per bunch, given by

$$N_b = \frac{I_{tot}}{e f_{rev} n_b} \tag{4}$$

with the revolution frequency f_{rev} and the maximum number of bunches n_b. The number of bunches cannot be arbitrary large due to the need for a minimal spacing between bunches (about 25 ns) in order to avoid adverse effects of electron clouds (Chap. **??**) as well as the needs for gaps for injection and extractions (Chap. **??**). This constraint is mostly relevant for the Z, yielding a minimum bunch charge of about $2 \cdot 10^{11}$ $e^{\pm}$/b. In the small crossing angle and large Piwinski angle approximation, the beam-beam parameters reduce to

$$\xi_x \approx \frac{N_b r_e}{\pi\gamma}\frac{2\beta_x^*}{(\sigma_z\theta)^2},\ \xi_x \approx \frac{N_b r_e}{\pi\gamma}\frac{1}{\sigma_z\theta}\sqrt{\frac{\beta_y^*}{\epsilon_y}}. \tag{5}$$

The bunch length is therefore a key parameter, it is driven by beamstrahlung, synchrotron radiation in the arcs, the RF strength and the choice of lattice, mainly through the momentum compaction factor. We can write

$$\sigma_z = \sigma_\delta\frac{\eta C_0}{2\pi Q_s},\ Q_s = \frac{1}{2\pi}\sqrt{\frac{eV_{RF}\omega_{RF}C_0}{P_0c^2}\eta\cos(\phi_s)},\ \sin(\phi_s) = \frac{\Delta E}{eV_{RF}} \tag{6}$$

with V_{RF} and ω_{RF} the RF voltage and frequency. C_0 is the machine circumference, P_0 the reference momentum, η the slippage factor and ΔE the total energy loss per turn. The synchrotron tune and synchronous phase are given by Q_s and ϕ_s. The momentum spread is given by

$$\sigma_\delta^2 = \sigma_{\delta,SR}^2 + \frac{n_{IP}\tau_{E,SR}c}{4C_0}\{n_\gamma\langle u^2\rangle_{BS}\},\ \text{with}\ \{n_\gamma\langle u^2\rangle_{BS}\} = \frac{55}{24\sqrt{3}}\frac{r_e^2\gamma^5}{\alpha_e}\int ds\left\langle\frac{1}{\rho^3}\right\rangle \tag{7}$$

where $\sigma_{\delta,SR}$ the r.m.s. relative momentum spread caused by synchrotron radiation in the arcs and $\tau_{E,SR}$ the corresponding damping time. n_{IP} is the number of IPs, α_e is the fine structure constant and ρ is the local bending radius of the particles' trajectories cause by the beam-beam interaction. Using strong assumptions, it is possible to approximate the integral over the bending radius as follows [**?**]

$$\int ds\left\langle\frac{1}{\rho^3}\right\rangle \approx \frac{0.77562}{\sqrt{2\pi}^3\sigma_z^2\phi}\left(\frac{2N_b r_e}{\gamma\sigma_x}\sqrt{\frac{2}{\pi}}\right)^3. \tag{8}$$

Using the equations above we write the equation for the momentum spread:

$$\sigma_\delta^5 - \sigma_{\delta,SR}^2\sigma_\delta^3 - \alpha_{BS} = 0,\ \alpha_{BS} \propto \frac{n_{IP}\tau_{E,SR}\gamma^{\frac{1}{2}}N_b^3}{\sigma_x^2\theta}\left(\frac{V_{RF}\omega_{RF}}{\eta}\right)^{\frac{3}{2}}, \tag{9}$$

the corresponding bunch length follows from Eq. 6. Due to its approximate nature, this equation is hardly used in the design and the impact of beamstrahlung is rather obtained via tracking simulations.

Yet this equation reveals that, in the regime of strong beamstrahlung ($\sigma_{\delta,BS} \ll \sigma_{\delta,SR}$) the sensitivity to RF parameters and momentum compaction factor is reduced from the usual square root dependence due to fact that the beam-beam force, and consequently the strength of beamstrahlung, is dependent on the bunch length. In the regime of strong beamstrahlung, we see that the main drivers for the bunch length and momentum spread are the bunch intensity and the horizontal beam size ($\sigma_\delta \propto N_b^{\frac{5}{3}} \sigma_x^{-\frac{5}{2}}$). These quantities must be adjusted to minimise beamstrahlung. As discussed above, the bunch intensity is constrained on the low side at the Z by the electron cloud instability. At the other energies it needs to be kept high enough to maintain the beam-beam parameter (and consequently the luminosity) at the specified level. Also, a low horizontal emittance is required to achieve a low vertical emittance. Indeed, the two quantities are bound by the quality of the optics correction, currently it is assumed that $\epsilon_y = 10^{-3}\epsilon_x$ can be achieved (Chap. **??**). The low vertical emittance enters directly in the luminosity, but is also important to maintain a good beam lifetime in the presence of a reduced vertical dynamic aperture that comes along with the low β_y^*. Thus, maintaining a high β_x^* is key to reduce beamstrahlung and maintain the horizontal beam size at the level of β_y^* in order to minimize the luminosity lost to the hourglass effect in the vertical plane, as discussed above. Nevertheless, the horizontal β^* is limited on the high side by the corresponding increase of the horizontal beam-beam parameter as well as of the strength of horizontal synchrobetatron resonances. These aspects are critical as the transverse tunes are set just above the half integer in the horizontal plan, above the coupling resonance and below the third order resonance in the vertical plane (Fig. 1), thus minimizing the impact of low order resonances on the beam quality. In this area, synchrobetatron sidebands of the half integer resonance in the horizontal plane are strongly excited due to the beam-beam interaction with a large Piwinski angle, leading to coherent instabilities, so-called X-Y instabilities [**?**], as well as incoherent blow up [**?**]. Consequently, the horizontal β^* must be chosen to maintain the strength of synchrobetatron resonances and the horizontal beam-beam parameter ($\xi_x \ll Q_s$) at an acceptable level. This optimisation, coupled to the relevant longitudinal aspects treated in the next paragraph, is done based on tracking simulation (Chap. **??**). Thanks to the increase in radiation damping and the shorter bunch length at higher energies, these effects become less severe and higher β_x^* are allowed.
The tune space depicted in Fig. 1 corresponds to the CDR configuration, yet the main features have not fundamentally changed. The main difference is the reduction of the tune per quarter of the machine (4 IPs layout), with respect to the half of the machine in the CDR (2 IPs layout) in order to maintain the total tune in the same area, thus avoiding important resonances when considering the impact of the real lattice (Fig. **??**). Approaching the half integer resonance is necessary to accommodate the twice larger total tune footprint with the 4 IPs layout with respect to the CDR.

The longitudinal parameters are set to ensure a sufficient bucket height, at the same time the spin tune spread needs to be remain sufficiently smaller that the synchrotron tune to allow for energy calibration via resonance depolarisation (Chap. **??**)

$$\left(\frac{\Delta p}{p}\right)_{max} = \sqrt{\frac{eV_{RF}\omega_{RF}C_0}{2\pi^2 c\eta E_0}(2\cos(\phi) + (2\phi_s - \pi)\sin(\phi_s))} > 0.01,\ Q_s > a\gamma\sigma_{\delta,SR} \qquad (10)$$

with a the anomalous magnetic moment. Aiming at a high voltage and low momentum compaction factor, maintaining a high synchrotron tune is therefore favourable. The available RF voltage is an important cost driver, it is therefore kept at the level required to compensate for the energy lost by synchrotron radiation maintaining a reasonably low synchronous phase. At the Z, an additional constraint on the RF voltage results from the choice of operating 2-cell cavities in reverse polarity mode in order to keep the same RF system for the Z, W and H energies (Chap. **??**). The voltage is kept higher than necessary to minimized the impact of transient beam loading.
Two different lattices are considered, one for the two highest energies (H and t) featuring a lower momentum compaction factor than the optics for the lower energies (Z and W). This different optics also allow to maintain low transverse emittances at higher energies.

While at the Z the number of bunches is constrained by the electron cloud instability, it can be optimised to obtained the highest luminosity at other energies. This is achieved by choosing the highest bunch charge that does not yields to too significant lifetime degradation or emittance growth ($\xi_y \approx 0.1$).

A key difference with existing colliders is the fact that beam parameters are defined by an equilibrium condition that it mostly driven by the beam-beam force itself. Transverse and longitudinal beam sizes are thus strongly coupled, bringing additional constraints on the design and operation of the collider. An important aspect is the need for a reasonably adiabatic ramp up of the beam-beam force, leading to the so-called bootstrap injection scheme (Chap. **??**). In a more classical scheme, where one beam would be circulating, and thus featuring the lattice equilibrium emittances, and a second beam injected with the equilibrium emittances define by the booster, the beam-beam force over the first turns would significantly exceed the acceptable strength ($\xi_y \gg 0.1$) causing uncontrolled beam losses and possibly leading to a 3D flip-flop mechanism before reaching the desired equilibrium with longer bunches and thus weaker beam-beam force.
The 3D flip-flop mechanism is a direct consequence of this strong coupling between the equilibrium in the different planes. In case of an asymmetry in the strength of beamstrahlung between the two colliding bunches, the bunch experiencing less beamstrahlung will see its length decrease, thus increasing the strength of beamstrahlung for the other beam. As a result, beamstrahlung will decrease further on the shorter bunch, thus enhancing further the effect. This setup may reach a stable equilibrium where the two bunches feature small enough asymmetries, yet this already results in a reduction of the luminosity with respect to the symmetric case [**?**]. Pushed beyond a certain threshold, the increase in the beam-beam force leads to beam losses and transverse emittance growth, thus enhancing the phenomenon in an irreversible manner, eventually causing one bunch to lose most of its intensity and blow up significantly while the other bunch experiences a vanishing beam-beam force and is thus let to shrink to the lattice equilibrium emittance. Avoiding this mechanism imposes tight tolerances on the symmetry of the two beams, in terms of bunch intensity and optics control in terms of β^* and equilibrium emittance.